Quantum Monte Carlo study of pressure-induced $B3$-$B1$ phase transition in GaAs

C. N. M. Ouma,[1,*] M. Z. Mapelu,[2] N. W. Makau,[2] G. O. Amolo,[2] and Ryo Maezono[3]

[1]*Physics Department, University of Pretoria, Pretoria 0002, South Africa,*

[2]*Computational Material Sciences Group, Chepkoilel University College, Department of Physics, P. O. Box 1125, Eldoret, Kenya*

[3]*School of Information Science, JAIST, Asahidai 1-1, Nomi, Ishikawa 923-1292, Japan*

(Received 10 April 2012; published 28 September 2012)

We have investigated the transition pressure p_t of bulk GaAs from the zinc-blende ($B3$) to the rocksalt ($B1$) structure using the local-density approximation (LDA), Perdew-Burke-Ernzerhof generalized gradient approximation (PBE-GGA), and diffusion Monte Carlo (DMC). We took into account finite temperature effects (zero-point vibrational effects) as well as finite-size corrections. Our DMC calculation using GGA trial nodal surface supports the higher value of the transition pressure, ∼17 GPa, than the lower value of ∼12 GPa, both of which are experimentally reported values. This projection increases the transition pressure p_t from DFT predictions, being of the same tendency as that for Si bulk crystal. The choice of the exchange-correlation functional in DFT was found to significantly determine the phase-transition pressure, while DMC gave more accurate results for this transition pressure.

DOI: 10.1103/PhysRevB.86.104115 PACS number(s): 61.48.Gh, 68.35.bg, 73.22.Pr

I. INTRODUCTION

There is rekindled interest in the study of high-pressure behavior of materials due to the advancement and refinements in the diamond-anvil cell technique (DAC). These studies have clearly shown that materials will exhibit new and interesting phase transitions and novel elastic behavior when subjected to pressure.[1] There has been an enormous amount of theoretical and experimental work on high-pressure phases and phase transitions done so far,[1–15] especially on GaAs, a binary group III-V semiconductor. This is mainly attributed both to its applications in microelectronic device fabrications and also its superior operational qualities to Si.[11]

Although experiments and theoretical investigations have successfully identified high-pressure phases of other semiconductors, uncertainties still abound on the high-pressure phase transitions of GaAs.[6] Different experiments and *ab initio* studies on pressure-induced phase transitions of GaAs have reported different transition pressure values[1,4–10,14,15] especially for the $B3$-$B1$ phase transition. High-pressure x-ray experiments[4,5] reveal that GaAs transforms from the fourfold-coordinated zinc-blende ($B3$) structure [see Fig. 1(a)] (GaAs-I) to a sixfold-coordinated (GaAs-II) structure at around 11.5–13.5 GPa,[5] and 17 GPa.[4] GaAs-II has been proposed to have the space group $Pmm2$,[4,5] which is a distortion of the rocksalt ($B1$) structure [see Fig. 1(b)].

Earlier *Ab initio* studies based on GGA and LDA functionals[1,11,12,14,15] predicted the $B3$-$B1$ pressure-induced phase transition in GaAs to occur at about 10.5,[11] 16.3,[12] 11.7,[14] 16.0,[15] and 17.0 GPa.[1] As seen in Table III, all the DFT predictions so far can be sorted into two values, those around 11 GPa and those around 16 GPa. It might seem to be accidental but these two seem to correspond to the two different experimental values. It is also well known that the choice of exchange-correlation (XC) functional strongly affects the DFT predictions. Known tendencies about this include that (1) lattice constants are underestimated (overestimated) by local-density approximation (LDA) [generalized gradient approximation (GGA)], and (2) bulk moduli are overestimated (underestimated) by LDA (GGA), and hence the true value is usually expected in between LDA and GGA predictions. It is, however, difficult to deduce such an "in between rule" for the transition pressures. A possible way to calibrate XC tendencies is to perform QMC evaluations. QMC, more specifically diffusion Monte Carlo (DMC), provides a more reliable evaluation of electron interactions not depending on XC functionals and also recently DMC has been used to calibrate transition pressures too.[16–20]

In this work we study the $B3$-$B1$ pressure-induced phase transition in GaAs using the highly accurate continuum quantum Monte Carlo (QMC) method.[21,22] We investigate whether the choice of charge density functionals as implemented in standard density functional theory (DFT) used so far to study this phase transition significantly affects the obtained phase-transition pressure, and also assess the accuracy of QMC in predicting the $B3$-$B1$ pressure-induced phase transition in GaAs.

This paper is organized as follows: Section I introduces the studies done so far on GaAs pressure-induced phase transiton, Sec. II outlines the basic theory of the computational methods used, Sec. III gives details on the methodology used, Sec. IV contains the results obtained and the discussion, while Sec. V gives the conclusions.

II. THEORY

First-principles calculations have made a significant contribution in describing the energetic, atomistic, and magnetic properties of materials. However, a significant test of these methods is the prediction of transition pressures.[1,6–15] Density functional theory (DFT) is the standard technique that has been used to probe the properties of materials at an *ab initio* level. DFT replaces the explicit many-body electron interactions with quasiparticles interacting via a mean-field potential [the exchange-correlation (XC) potential]. This XC potential is a functional of the charge density.[23–25] However, there is no known universally true XC functional, thus DFT studies normally employ approximate functionals based on diffusion Monte Carlo (DMC) calculations[26] for the homogeneous electron gas at different charge densities [the local-density

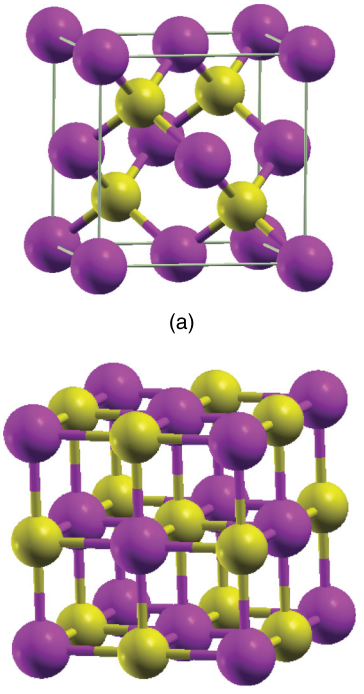

FIG. 1. (Color online) GaAs structures: (a) $B3$ (zinc-blende)-GaAs structure; (b) $B1$ (rocksalt)-GaAs structure. Magenta spheres are Ga atoms and golden ones are As atoms.

approximation (LDA)][27,28] or gradient expansions [generalized gradient approximations (GGAs)].[29–33] Studies have shown that these functionals (LDA and GGA) possess self-interaction errors as reflected in the accuracy of their predictions of band gaps;[34] case in point, the GGA functional predicts germanium (Ge), which is a semiconductor, to be metallic.[35]

Improved computational accuracy can be achieved with the continuum quantum Monte Carlo (QMC) technique.[21,22] QMC methods, namely, diffusion Monte Carlo and variation Monte Carlo (VMC), are stochastic *ab initio* techniques for solving the many-body Schrödinger equation. Their accuracy compared to that of post-Hartree-Fock quantum chemistry techniques has been confirmed by various studies (see Refs. 21, 22, and 36, and the references therein). QMC techniques, however, have in the recent past been expensive, which limited their applicability to different systems but with the increase in computing power it is now possible to use QMC techniques to probe systems that were previously intractable. DMC has accurately predicted solid-state structural phase transitions,[16–18,35,37] hence the motivation of this study.

VMC is a stochastic way of evaluating the expectation value of the Hamiltonian of the system, while DMC is a stochastic way of solving the Schrödinger equation in imaginary time. DMC exactly projects the ground state of the system in the limit of long imaginary time. However, practical calculations require the introduction of approximations which include the fixed-node approximation, an approximation related to the antisymmetry of the wave function where the wave function changes sign, and an approximation due to the need for replacing the Coulomb potential generated by the nuclei of heavy atoms with a pseudopotential.[21,22]

III. COMPUTATIONAL METHOD AND DETAILS

A. DFT calculations

Norm conserving pseudopotentials for As $4s^2 4p^3$ and Ga $3d^{10} 4s^2 4p^1$ within the GGA and LDA formalisms were used to perform the DFT calculations for the two structures of GaAs shown in Fig. 1. Trail-Needs smooth relativistic pseudo potentials are used.[38] For both Ga and As we chose the s channel as the local part so as to prevent the ghost state problem. The Brillouin zone was sampled with a Monkhorst-Pack (MP)[39] grid of k points. To reduce the finite-size error on kinetic energies, we used an MP mesh shifted to the L point.[18,40–42] Convergence tests were done on all the structures based on the MP grid and for plane-wave cutoff energy, to an accuracy of 10^{-6} Ry in the computed total energies. Converged plane-wave cutoff energies of 50 Ry and a $12 \times 12 \times 12$ MP grid was chosen for both the $B3$ and $B1$ structures. The DFT calculations were performed using the QUANTUM ESPRESSO code.[43] In order to ensure that the volumes used for finding the phase-transition pressure were stable, we performed phonon calculations, as implemented in the QUANTUM ESPRESSO code,[43] on each of the volumes.

B. Phonon contribution

We also investigated the effect of changing temperature from 0 to 300 K. To do this one has to look at the free energy, incorporating the effects of phonons. The free energy at temperature T and lattice constant a is given, within the quasiharmonic approximation, by

$$F(a,T) = E_{\text{stat}}(a) + k_B T \sum_{\mathbf{q}\lambda} \ln \left\{ 2 \sinh \left(\frac{\hbar \omega_{\mathbf{q}\lambda}(a)}{2 k_B T} \right) \right\}. \quad (1)$$

The first term on the right-hand side is the static energy $E_{\text{stat}}(a)$, while the second term is the vibrational free energy. The sum is over all three phonon branches λ and over all wave vectors $\mathbf{q}$ in the Brillouin zone (BZ). $\hbar$ is the Planck constant, k_B is the Boltzmann constant, and $\omega_{\mathbf{q}\lambda}(a)$ is the frequency of the phonon wave vector $\mathbf{q}$, which is evaluated at lattice constant a. At a constant temperature T, the lattice constant $a_0(T)$ can be obtained via minimizing $F(a,T)$ with respect to a. We then evaluated the total energies at a range of lattice constants for 0 and 300 K. Phonon dynamical matrices were computed for a $8 \times 8 \times 8$ $\mathbf{q}$-point mesh at each lattice constant. Fourier interpolation was then used to obtain the dynamical matrices on a $36 \times 36 \times 36$ $\mathbf{q}$-point mesh. These dynamical matrices were then used to evaluate all quantities that involve an integration over phonon wave vectors $\mathbf{q}$ as implemented in the QUANTUM ESPRESSO code.[43]

C. QMC calculations

The QMC (VMC and DMC) calculations were performed using the CASINO code.[21,22] We used trial wave functions of Slater-Jastrow types. The Slater-Jastrow form is

$$\Psi_{\text{SJ}}(\mathbf{R}) = \exp[J(\mathbf{R})] \det[\psi_n(\mathbf{r}_i^{\uparrow})] \det[\psi_n(\mathbf{r}_j^{\downarrow})], \quad (2)$$

where $\mathbf{R}$ denotes the positions of all the electrons, $\mathbf{r}_i^{\uparrow}$ is the position of the ith spin-up electron, $\mathbf{r}_j^{\downarrow}$ is the position of the jth spin-down electron, $\exp[J(\mathbf{R})]$ is the Jastrow

factor, and $\det[\psi_n(\mathbf{r}_i^{\uparrow})]$ and $\det[\psi_n(\mathbf{r}_i^{\downarrow})]$ are determinants of single-particle orbitals. The orbitals were generated by QUANTUM ESPRESSO using Perdew-Burke-Ernzerhof (PBE)-GGA functionals. The conditions are the same as DFT calculations described earlier except for the reduced grid size of $4 \times 4 \times 4$ that corresponds to a QMC simulation cell size of 512 electrons (128 atoms) for $B1$ and $B3$ structures without magnetic polarizations. The orbitals were then transformed into a B-spline or "blip" polynomial basis for greater efficiency.[44] The nonlocal pseudopotential energy was calculated using the variational scheme of Ref. 45 (i.e., T-move scheme). We used Jastrow factors consisting of polynomial electron-nucleus (en) and electron-electron (ee) terms[46] with a total of 32 optimizable parameters. The wave-function parameters were optimized by a variational Monte Carlo (VMC) procedure in which we minimized the variance of the energy.[47,48]

Because of the computational resource limitation, QMC only manages to treat hundreds to a thousand electrons even with up-to-date high performance computing.[18] Smaller simulation cells, such as $4 \times 4 \times 4$, when used to model infinite-size systems by the periodic boundary conditions inevitably introduces the finite-size errors. To correct for these errors there are several schemes available.[22] The finite-size effect error due to the electron-electron interaction can be estimated by comparing the results of Ewald interaction and those of the model Coulomb potentials (MPCs).[42,49,50] For metallic systems, such as the $B1$ phase in the present case, the error in the kinetic energies is also sensitive. This error can be reduced by adjusting the k-point mesh. A shifted k-point mesh generally requires complex many-body wave functions for QMCs. A more sophisticated method is averaging over the choice of the shift, corresponding to the average over twisting boundary conditions.[18] We did not take into account the twisting average in the present study, but only used a shifted k-point mesh.[18]

We used a target population of 640 configurations in each of our DMC calculations. All of the results reported here were obtained using a DMC time step $\Delta\tau$ of 0.01 a.u. The time step should be carefully chosen when one uses the T-move scheme because it is known to introduce larger time-step errors. We investigated the biases of the ground-state energies at equilibrium volumes as a function of the DMC time steps $\Delta\tau$, and confirmed that they are within the statistical error bars for both structures with and without T-move scheme, as shown in Fig. 2.

D. Phase-transition pressure

After the phonon correction, see Eq. (1), we got F-V dependence, which is subject to the fitting of the equation of state (EoS). There exist several proposed forms of the EoS, such as the Murnaghan,[51] Birch-Murnaghan,[52] Vinet,[53] Dodson,[54] Kumari-Dass,[55] and Parsafar-Mason[56] EoSs. We have chosen Vinet EoS,

$$F(V) = -\frac{4B_0V_0}{(B_0^{'}-1)^2}\left\{1-\frac{3}{2}(B_0^{'}-1)\left[1-\left(\frac{V}{V_0}\right)^{1/3}\right]\right\} \times \exp\left\{\frac{3}{2}(B_0^{'}-1)\left[1-\left(\frac{V}{V_0}\right)^{1/3}\right]\right\} + C, \quad (3)$$

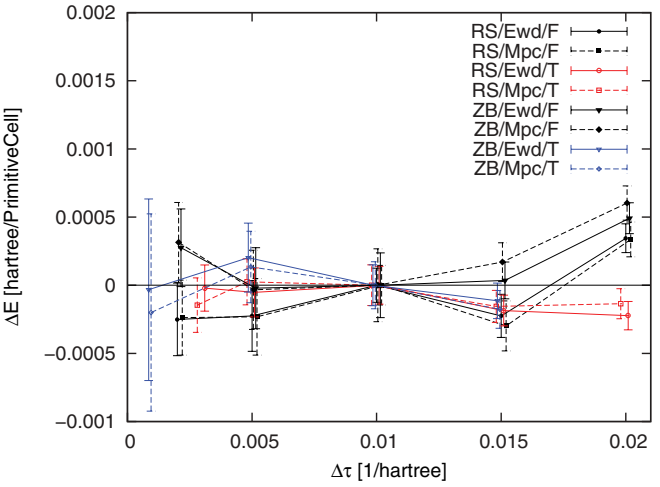

FIG. 2. (Color online) Biases of the ground-state energies at equilibrium volumes of $B1$ (RS) and $B3$ (ZB) structures depending on the DMC time steps (dtdmc), measured from those obtained by dtdmc = 0.01 a.u. Plot points are shifted by a tiny amount along horizontal axis just for visibility. "Mpc/Ewd" means the schemes to evaluate Coulombic interactions, model Coulomb potentials (MPCs), and Ewald scheme, respectively. "T" and "F" specify that the variational scheme in Ref. 45 (T-move scheme) is used (T) or not (F).

in the present work because it has shown most robust behaviors of fitting in previous works.[18,57,58] For QMC data with standard errors, the bulk parameters as statistical estimates were evaluated as follows: The Gaussian noises with the standard deviation σ being the same value as that of QMC data at each volume were generated and added to the mean value of QMC. Then the bulk parameters were fitted by χ^2-estimation scheme. Repeating this procedure with random noises gives a set of fitted parameters as random variables, from which the error bars of the fitted parameters were calculated.

Since the pressure is given by

$$P = -\frac{\partial F}{\partial V}, \quad (4)$$

the phase-transition pressure can be obtained as the common tangent of two EoSs of each phase, the $B1$ and $B3$ phase in the present case, as shown in Fig. 4.

IV. RESULTS AND DISCUSSION

A. Bulk properties

Tables I and II summarize the bulk properties of GaAs obtained using LDA, GGA, and QMC calculations. These are compared with previous *ab initio* studies[10–12] as well as the experimental ones. Note that there are no experimental values for $B1$-GaAs. We also note that the results for $T = 0$ K in Table I take into account the zero-point energies estimated by phonon force-constant evaluations, as included in Eq. (1).

For fourfold coordinated zinc-blende (ZB) structure, present DMC results gives the tendency in calibrating DFTs as $a_0^{(\mathrm{GGA})} > a_0^{(\mathrm{LDA})} \sim a_0^{(\mathrm{DMC})}$ for lattice constants, and $B_0^{(\mathrm{DMC})} > B_0^{(\mathrm{LDA})} > B_0^{(\mathrm{GGA})}$ for bulk modulus. The same tendency is

TABLE I. Calculated bulk properties of $B3$ and $B1$ structures of GaAs estimated by Vinet EoS at $T = 0$ K. The values in parentheses for QMC data mean the statistical errors in the last digit, such as $5.72(4) = 5.72 \pm 0.04$.

Structure		a_0 (Å)	B_0 (GPa)	$B_0^{'}$	
$B3$ (zinc blende)		5.7337	64.08	6.23	GGA 12×12×12
		5.7173	68.29	5.91	LDA 12×12×12
		5.7167(5)	82.89(4)	2.3(1)	DMC Ewald
		5.7162(6)	80.48(5)	2.8(3)	DMC MPC
	Other calc.	5.56[a]	79.75[a]	3.5[a]	
		5.648[b]	76.03[b]	3.9[b]	
		5.61[e]	74[e]	4.6[e]	
		5.58,[d] 5.567[d]	75.2,[d] 78.1[d]		
	Expt.	5.653[c]	75.7[c]	4[c]	
$B1$ (rocksalt)	This work	5.3606	76.62	4.09	GGA 12×12×12
		5.3434	80.92	4.53	LDA 12×12×12 (Vinet)
		5.354(1)	67.49(3)	2.27(5)	DMC Ewald
		5.354(1)	70.45(3)	2.15(5)	DMC MPC
	Other calc.	5.28[a]	69.95[a]	4.87[a]	
		5.31[b]	95.63[b]	4.05[b]	
		5.23,[d] 5.208[d]	90.1,[d] 95.1[d]		

[a]Reference 12.
[b]Reference 11.
[c]Reference 59.
[d]Reference 13.
[e]Reference 9.

reported in the case of Si diamond[18,19,37] and Si cluster.[58] For carbon (in diamond structure),[57] both $a_0^{(\mathrm{DMC})}$ and $B_0^{(\mathrm{DMC})}$ are in between GGA and LDA. For the sixfold coordinated rocksalt (RS) structure, the calibrations are $a_0^{(\mathrm{LDA})} < a_0^{(\mathrm{DMC})} < a_0^{(\mathrm{GGA})}$ and $B_0^{(\mathrm{LDA})} > B_0^{(\mathrm{GGA})} > B_0^{(\mathrm{DMC})}$. For B_0, this is opposite to the sixfold coordinated Si β-tin case.[18] When we look at the results at finite temperature, Table II, we could draw the tendency that LDA is better (closer to DMC reference) for the insulating phase (ZB) and GGA for the metallic phase (RS). We also notice that the finite-size correction, as the change from Ewand to MPC, makes the DMC predictions on B_0 closer to DFT values by decreasing (increasing) them for ZB (RS). The opposite directions of the correction for ZB and RS would imply that the long-ranged nature of the interaction fictitiously feeling the edge of the simulation cell gives opposite effects on the modulus depending on the structure.

Comparing with the experimental bulk modulus for ZB, Tables I and II show that DMC's projection operation corrects our DFT estimation closer to the experimental one. It is observed as well that the finite-size correction by MPC contributes significantly to this "approaching."

For lattice constants, our present study tends to overestimate them. DMC seems to retain the overestimated values in our DFT results. In order to see if the overestimation comes from our pseudopotentials, we did DFT calculations using the same pseudopotentials with Heyd, Scuseria, and Erzenhof (HSE06) (Ref. 60) hybrid functionals, and obtained a lattice constant of 5.67 Å for ZB structure while we obtained 5.73 Å using GGA. The results are consistent with those obtained by a full potential DFT,[36] reporting 5.66 Å (5.743 Å) in HSE (GGA). This might imply that our pseudopotentials have little cause for the overestimation. Yet, another PBE-GGA reported a value of 5.56 Å:[12] They got this with ul-

TABLE II. Calculated bulk properties of $B3$ and $B1$ structures of GaAs estimated by Vinet EoS at $T = 300$ K. The values in parentheses for QMC data mean the statistical errors in the last digit, such as $5.72(4) = 5.72 \pm 0.04$.

Structure		a_0 (Å)	B_0 (GPa)	$B_0^{'}$	
$B3$ (zinc blende)		5.7411	61.45	6.26	GGA 12×12×12
		5.7234	65.86	5.78	LDA 12×12×12
		5.7216(5)	81.06(4)	2.3(1)	DMC Ewald
		5.7220(6)	78.65(5)	2.7(3)	DMC MPC
	Expt.	5.653[a]	75.7[a]	4[a]	
$B1$ (rocksalt)	This work	5.3927	60.53	7.03	GGA 12×12×12
		5.3687	69.90	5.35	LDA 12×12×12
		5.391(2)	58.93(3)	2.20(6)	DMC Ewald
		5.388(2)	62.07(3)	2.10(5)	DMC MPC

[a]Reference 59.

trasoft potentials with the same core size as ours but with rather smaller $8 \times 8 \times 8$ mesh size. From these findings, we cannot give a definite conclusion of the overestimation here, at least compared with Ref. 12. It has also been reported that the equilibrium lattice constant is affected by the configuration chosen during the pseudopotential generation. For GaAs it is reported that the equilibrium lattice constant is sensitively affected by the form of $3d$ potential of Ga because of the p-d interaction.[14] They (Ref. 14) report that the configuration chosen when the pseudopotential is generated may change the lattice constant by 1–2%, which is the same amount as our deviations.

We plucked out the volumes with imaginary frequencies estimated at DFT level to get the final parametrization of the EoS for both DFT and QMC. We have confirmed, however, that the results do not change so much when we included the plucked volumes. The QMC data by the trial nodes with imaginary frequencies at the plucked volumes are well fitted by the EoS obtained with plucking these data.

B. Phase-transition pressure

Table III summarizes the calculated transition pressure p_t between $B3$ and $B1$ structures of GaAs. Note again that $T = 0$ K results take into account the zero-point vibration. Figure 4 shows common tangents to get p_t for DMC data. Apart from LDA ('87) data in Table III, one can notice the tendency of preceding DFT works predicting smaller p_t (around 11 GPa) by LDA and larger (around 16 GPa) by GGA. Our present DFT results are consistent with this tendency. From Fig. 3 one can understand why GGA gives larger p_t than LDA: that is partly because of the E-V dependence of ZB structure which is predicted to be more stable in GGA when the volume is increased from the compressed region, thus getting more gradient for the common tangent, though it is also affected by the relative energy difference between the ZB and RS structures.

TABLE III. Calculated $B3$-$B1$ phase-transition pressure (p_t) in GPa. "MIP" and "TBP" stand for Mobius inversion potentials and three-body potential, respectively. The values in parentheses for QMC data mean the statistical errors in the last digit, such as $5.72(4) = 5.72 \pm 0.04$.

	p_t		
This work	13.46	0 K	GGA 12×12×12
	9.61	0 K	LDA 12×12×12
	16.8(8)	0 K	DMC Ewald
	17.3(8)	0 K	DMC MPC
	13.07	300 K	GGA 12×12×12
	9.08	300 K	LDA 12×12×12
	16.3(7)	300 K	DMC Ewald
	16.8(8)	300 K	DMC MPC
Expt.	12 ± 1.50		Ref. 4
	17.00		Ref. 5
Other calc.	16.00	LDA ('87)	Ref. 15
	11.70	LDA ('93)	Ref. 14
	13.00	LDA (95)	Ref. 9
	10.50	LDA ('08)	Ref. 11
	16.30	GGA ('06)	Ref. 12
	11.80	MIP	Ref. 13
	17.00	TBP	Ref. 1

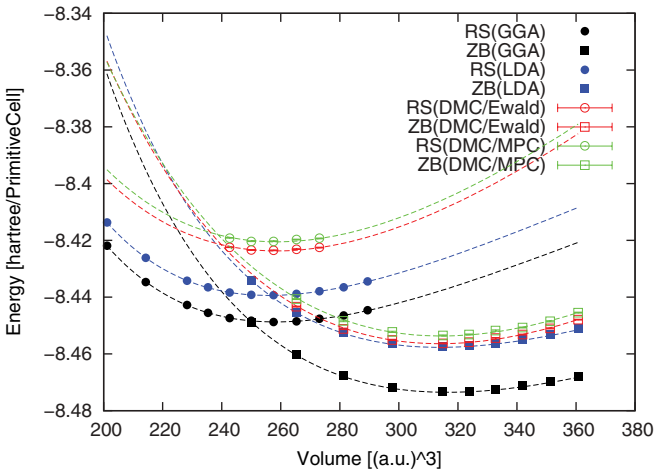

FIG. 3. (Color online) Energy-volume dependence (without phonon contribution) evaluated by DFT and DMC energy for $B3$ (zinc-blende; squared symbols) and $B1$ (rocksalt; circle symbols) structures of GaAs. Variation of total energy vs volume for $B3$ (zinc-blende) and $B1$ (rocksalt) structures of GaAs. The volumes with imaginary phonon frequencies are included for DFT data. Statistical error bars for QMC data shown are within the size of each symbol.

The present DMC study predicts larger p_t than that by DFT, i.e., $p_t^{(\mathrm{LDA})} < p_t^{(\mathrm{GGA})} < p_t^{(\mathrm{DMC})}$. This calibration tendency is also reported in the Si diamond to β-tin transition case.[18] In the Si case, larger $p_t^{(\mathrm{DMC})}$ is regarded as an overestimation compared with experiments. In the present case it depends on which experimental value is referred to, i.e., 12 GPa,[4] or 17 GPa.[5] Again from Fig. 3 one can understand why DMC gives larger p_t than DFT: DMC corrects the energy of the RS phase upward with a larger amount than that of the ZB phase. The magnitude of the common tangent p_t thus increases. This implies that DMC corrects "higher density/metallic" phase more than "lower density/insulating" phase. This would be in contrast to the naive expectation, namely, LDA based functionals get better for higher density. We could not, however, account for why the present DMC gives a larger energy shift from DFT in the higher density phase.

A finite-size correction appears to shift the prediction to larger p_t values. From Fig. 4 one can conclude that the finite temperature effect gives almost a parallel shift of the common tangent, giving a little reduction of the predicted p_t closer to experimental ones. Free energies of each phase are increased by taking into account zero-point vibration, but are decreased again by raising the temperature because of the TS term, where S is the entropy and T is the temperature. The entropy S is expected to be large for the sixfold-coordinated RS phase due to a larger number of bondings than fourfold-coordinated ZB. Thus the free-energy reduction is expected to be larger in the RS phase compared to the ZB phase, hence the magnitude of the common tangent, p_t, decreases with increase in temperature T.

Using GGA a transition pressure $p_t = 13.67$ GPa was obtained, while DMC calculations gave a value of 16.3 GPa.

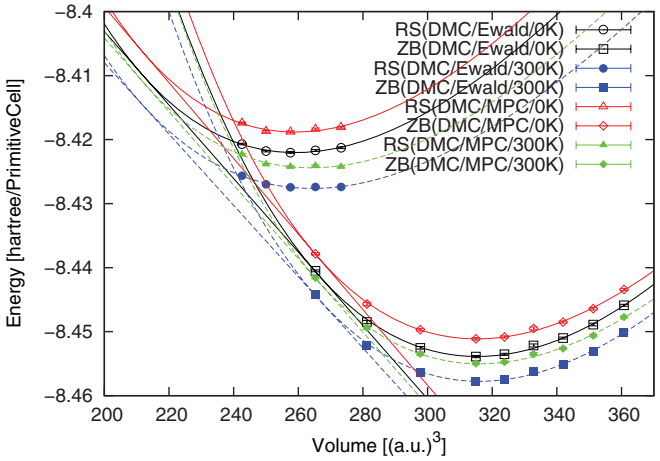

FIG. 4. (Color online) Energy-volume dependence of DMC energy for $B3$ (zinc-blende; squared symbols) and $B1$ (rocksalt; circle symbols) structures of GaAs. Solid lines correspond to $T = 0$ K and dashed ones to $T = 300$ K, both of which include phonon contributions. Black and blue lines correspond to Ewald evaluation and red and green to MPC. Statistical error bars for QMC data shown are within the size of each symbol.

This is in contrast to the result by Ref. 12 who reported a p_t value of 16.3 GPa using PBE-GGA itself. They used ultrasoft pseudopotentials with the same size of cores, and the k-mesh size of $8 \times 8 \times 8$, evaluating enthalpy. The transition is obtained as the crossing of enthalpy curves for RS and ZB to get p_t. They then evaluated the zero-point vibration using the QHD (quasiharmonic Debye) model.

We note in Figs. 3 and 4 that high-pressure phases often show imaginary phonon frequencies corresponding to instability of the structure. We have plucked out such volumes with imaginary phonon frequencies, in the $B1$ (RS) phase, as seen in Fig. 4, which has reduced data points compared with those in Fig. 3. The plucking as confirmed in this study gave little changes on the predicted bulk properties as well as the transition pressure. We also tried careful phonon calculations taking into account the acoustic sum rule in order to see if the imaginary phonon modes are spurious ones typically appearing near the Γ point, however, these imaginary modes proved to be intrinsic. We also note that in our trial calculations for the CsCl ($B2$)-GaAs structure, all the volumes were suffering from this imaginary phonon frequencies problem: we could in principle, evaluate "a formal estimation" p_t for the $B1$-$B2$ transition as well because, just as in Fig. 3, our CsCl structure gave a smooth E-V curve, but with imaginary phonon frequencies. Although there are several previous reports treating the $B1$-$B2$ transition by DFT,[9] we cannot find, to the best of our knowledge, any investigation using phonon stability.

C. Instabilities of structures at metallic phase

When we compare Figs. 3 and 4 we notice that the present calculation implies a structural transition from the $B3$ structure into an unstable lattice structure. As described in the Introduction, the high-pressure phase, GaAs-II, is not fully identified as a $B1$ structure but rather a slight distortion of the $B1$ structure. We do not know if the instability can be attributed to this, but we suspect that this is rather an artifact of DFT phonon evaluation with harmonic and adiabatic approximations. The same instability problem is reported in the Si pressure-induced phase transition from diamond to β-tin structure,[18,35,37] where the high-pressure structure (β-tin) is also metallic, similar to our $B1$ structure case.[9] We have carefully investigated the dependence on the grid coarseness of k mesh but we found that the instability of the structure does not disappear even if we used a dense mesh. Even though we cannot conclusively give a definite reason for this, the degenerate nature of the metallic phase might be playing a role, since, for metallic systems, there are actually very many degenerated states near the ground state (GS). The smearing procedure forces the system to sit in one of such degenerated states, which might actually be an excited state with infinitesimal excitation energy from true GS. In such a case, it might be possible to observe instability in phonon excitations. We also note that the imaginary frequencies occur at nonzero wave vector. All the formalisms used to evaluate phonon in DFT are based on the adiabatic approximation, which is anchored on the assumption that the dynamics of phonons are sufficiently slower than that of electrons. This assumption worsens with the increase in the kinetic energy of phonons.

V. CONCLUSION

We have performed DFT and QMC studies on the pressure-induced phase transition of GaAs from the fourfold coordinated $B3$ (zinc-blende) structure to the sixfold coordinated $B1$ (rocksalt) structure. It is shown that the DMC projection from DFT calibrates the transition pressure p_t to a higher value than DFT predicts. The dependence on exchange-correlation functionals in the bulk properties and the transition pressure within DFT is consistent with earlier studies apart from that by Zhang *et al.*[15] as shown in Tables I and II. The tendency of DMC calibrations over DFT for the present GaAs case is consistent with those for Si bulk properties and the transition pressure.[18,19,37] The shift by DMC calibration is established as resulting from the larger correction for the energy of metallic phase (higher density phase) than that of lower density phase, making the common tangent on the dependence of free energies on system volumes steeper. We have investigated the phonon contributions to the prediction. It is also established in this work that, at higher compression, the system suffers from imaginary phonon frequencies showing that the structure is unstable, though the energy values in such regions behave smoothly. By this careful examination we concluded that it is not possible to treat the transition pressure for $B1$-$B2$ (rocksalt-CsCl) structures unless the imaginary phonon frequencies problem is resolved. For more realistic comparison with experiments, we have estimated the transition pressure at $T = 300$ K. Finite-temperature effect, within our framework (DFT correction with quasiharmonic approximation), corrects the transition pressure by a little reduction. This is attributed to the higher entropy in the sixfold coordination in the RS structure than the fourfold coordinated ZB structure, accounting for more reduction of the free energy through the entropy term $-TS$, making the common tangent

less steep. Accompanied with the finite-size correction for the interaction part, our DMC-MPC at 300 K gives the transition pressure being quite consistent with an experimental value reporting 17.00 GPa.

ACKNOWLEDGMENTS

This work was supported by the Kenya National Council for Science and Technology (NCST) Grant No. NCST/5/003/0241, and the Computational Materials Sciences Group, Department of Physics, Chepkoilel University College, Eldoret-Kenya. One of the authors, C.N.M.O., wishes to acknowledge the Center for High Performance Computing (CHPC) in Cape Town, South Africa for computational resources. R.M. appreciates the financial support by a Grant in Aid for Scientific Research on Innovative Areas "Materials Design through Computics: Complex Correlation and Non-Equilibrium Dynamics" (Grant No. 22104011), "Optical Science of Dynamically Correlated Electrons" (Grant No. 23104714) of the Ministry of Education, Culture, Sports, Science, and Technology (KAKENHI-MEXT/Japan), and Tokuyama Science Foundation.

*Cecil.Ouma@up.ac.za

[1] R. K. Singh and S. Sadhna, Phys. Rev. B **39**, 671 (1989).
[2] G. Ackland, Rep. Prog. Phys. **64**, 483 (2001).
[3] S. Froyen and M. Cohen, Phys. Rev. B **28**, 3258 (1983).
[4] S. Weir, Y. Vohra, C. Vanderborgh, and A. Ruoff, Phys. Rev. B **39**, 1280 (1989).
[5] J. Besson, J. Itie, A. Polian, G. Weill, J. Mansot, and J. Gonzalez, Phys. Rev. B **44**, 4214 (1991).
[6] M. Durandurdu and D. Drabold, Phys. Rev. B **66**, 045209 (2002).
[7] M. McMahon and R. Nelmes, Phys. Status Solidi B **198**, 389 (2006).
[8] M. McMahon and R. Nelmes, Phys. Rev. Lett. **78**, 3697 (1997).
[9] A. Mujica, R. Needs, and A. Munoz, Phys. Rev. B **52**, 8881 (1995).
[10] A. Mujica, A. Munoz, and R. Needs, Phys. Rev. B **57**, 1344 (1998).
[11] D. Gupta and S. Kulshrestha, J. Phys.: Condens. Matter **20**, 255204 (2008).
[12] L. Lai-Yu, C. Xiang-Rong, Y. Bai-Ru, and G. Qing-Quan, Chin. Phys. **15**, 802 (2006).
[13] J. Cai, N. Chen, and H. Wang, J. Phys. Chem. Solids **68**, 445 (2007).
[14] A. Garcia and M. L. Cohen, Phys. Rev. B **47**, 6751 (1993).
[15] S. Zhang and M. Cohen, Phys. Rev. B **35**, 7604 (1987).
[16] D. Alfè, M. Gillan, M. Towler, and R. Needs, Phys. Rev. B **70**, 214102 (2004).
[17] D. Alfè, M. Alfredsson, J. Brodholt, M. J. Gillan, M. D. Towler, and R. J. Needs, Phys. Rev. B **72**, 014114 (2005).
[18] R. Maezono, N. Drummond, A. Ma, and R. Needs, Phys. Rev. B **82**, 184108 (2010).
[19] R. Hennig, A. Wadehra, K. Driver, W. Parker, C. Umrigar, and J. Wilkins, Phys. Rev. B **82**, 014101 (2010).
[20] D. Alfè, Rev. Miner. Geochem. **71**, 337 (2010).
[21] M. Towler, Phys. Status Solidi B **243**, 2573 (2006).
[22] R. Needs, M. Towler, N. Drummond, and P. López Ríos, J. Phys.: Condens. Matter **22**, 023201 (2010).
[23] P. Hohenberg and W. Kohn, Phys. Rev. **136**, B864 (1964).
[24] W. Kohn and L. J. Sham, Phys. Rev. **140**, A1133 (1965).
[25] W. Kohn, A. Becke, and R. Parr, J. Phys. Chem. **100**, 12974 (1996).
[26] D. Ceperley and B. Alder, Phys. Rev. Lett. **45**, 566 (1980).
[27] J. Perdew and A. Zunger, Phys. Rev. B **23**, 5048 (1981).
[28] J. Perdew and Y. Wang, Phys. Rev. B **45**, 13244 (1992).
[29] J. Perdew, Physica B **172**, 1 (1991).
[30] J. Perdew, K. Burke, and M. Ernzerhof, Phys. Rev. Lett. **77**, 3865 (1996).
[31] R. Armiento and A. Mattsson, Phys. Rev. B **72**, 085108 (2005).
[32] Z. Wu and R. Cohen, Phys. Rev. B **73**, 235116 (2006).
[33] J. Perdew, A. Ruzsinszky, G. Csonka, O. Vydrov, G. Scuseria, L. Constantin, X. Zhou, and K. Burke, Phys. Rev. Lett. **100**, 136406 (2008).
[34] R. Nieminen, Modell. Simul. Mater. Sci. Eng. **17**, 084001 (2009).
[35] E. Batista, J. Heyd, R. Hennig, B. Uberuaga, R. Martin, G. Scuseria, C. Umrigar, and J. Wilkins, Phys. Rev. B **74**, 121102 (2006).
[36] M. Schlipf, M. Betzinger, C. Friedrich, M. Ležaić, and S. Blügel, Phys. Rev. B **84**, 125142 (2011).
[37] S. Sorella, M. Casula, L. Spanu, and A. Dal Corso, Phys. Rev. B **83**, 075119 (2011).
[38] J. Trail and R. Needs, J. Chem. Phys. **122**, 174109 (2005).
[39] H. Monkhorst and J. Pack, Phys. Rev. B **13**, 5188 (1976).
[40] G. Rajagopal, R. Needs, S. Kenny, W. Foulkes, and A. James, Phys. Rev. Lett. **73**, 1959 (1994).
[41] G. Rajagopal, R. Needs, A. James, S. Kenny, and W. Foulkes, Phys. Rev. B **51**, 10591 (1995).
[42] P. Kent, R. Hood, A. Williamson, R. Needs, W. Foulkes, and G. Rajagopal, Phys. Rev. B **59**, 1917 (1999).
[43] P. Giannozzi, S. Baroni, N. Bonini, M. Calandra, R. Car, C. Cavazzoni, D. Ceresoli, G. Chiarotti, M. Cococcioni, I. Dabo *et al.*, J. Phys.: Condens. Matter **21**, 395502 (2009).
[44] D. Alfè and M. Gillan, Phys. Rev. B **70**, 161101 (2004).
[45] M. Casula, Phys. Rev. B **74**, 161102 (2006).
[46] N. Drummond, M. Towler, and R. Needs, Phys. Rev. B **70**, 235119 (2004).
[47] C. Umrigar, K. Wilson, and J. Wilkins, Phys. Rev. Lett. **60**, 1719 (1988).
[48] N. Drummond and R. Needs, Phys. Rev. B **72**, 085124 (2005).
[49] A. Williamson, G. Rajagopal, R. Needs, L. Fraser, W. Foulkes, Y. Wang, and M. Chou, Phys. Rev. B **55**, R4851 (1997).
[50] L. Fraser, W. Foulkes, G. Rajagopal, R. Needs, S. Kenny, and A. Williamson, Phys. Rev. B **53**, 1814 (1996).
[51] F. Murnaghan, Proc. Natl. Acad. Sci. USA **30**, 244 (1944).
[52] F. Birch, J. Geophys. Res. **52**, 227 (1952).
[53] P. Vinet, J. Ferrante, J. Smith, and J. Rose, J. Phys. C **19**, L467 (1986).
[54] B. Dodson *et al.*, Phys. Rev. B **35**, 2619 (1987).
[55] M. Kumari and N. Dass, J. Phys.: Condens. Matter **2**, 3219 (1990).
[56] G. Parsafar and E. Mason, Phys. Rev. B **49**, 3049 (1994).
[57] R. Maezono, A. Ma, M. Towler, and R. Needs, Phys. Rev. Lett. **98**, 025701 (2007).
[58] R. Cherian, C. Gerard, P. Mahadevan, N. Cuong, and R. Maezono, Phys. Rev. B **82**, 235321 (2010).
[59] R. C. Weast, *Handbook of Chemistry and Physics* (Rubber Co, Cleveland, 1970).
[60] K. Hummer, J. Harl, and G. Kresse, Phys. Rev. B **80**, 115205 (2009).